N72-33946

NASA TECHNICAL NOTE

NASA TN D-6956

NASA TN D-6956

CASE FILE COPY

FLIGHT AND GROUND TESTS OF A VERY-LOW-DENSITY ELASTOMERIC ABLATIVE MATERIAL

by George C. Olsen and Andrew J. Chapman III

Langley Research Center
Hampton, Va. 23365

NATIONAL AERONAUTICS AND SPACE ADMINISTRATION • WASHINGTON, D. C. • NOVEMBER 1972

1. Report No.	2. Government Accession No.	3. Recipient's Catalog No.
NASA TN D-6956		

4. Title and Subtitle	5. Report Date
FLIGHT AND GROUND TESTS OF A VERY-LOW-DENSITY ELASTOMERIC ABLATIVE MATERIAL	November 1972
	6. Performing Organization Code
7. Author(s)	8. Performing Organization Report No.
George C. Olsen and Andrew J. Chapman III	L-8412
	10. Work Unit No.
9. Performing Organization Name and Address	502-37-02-01
NASA Langley Research Center Hampton, Va. 23365	11. Contract or Grant No.
	13. Type of Report and Period Covered
12. Sponsoring Agency Name and Address	Technical Note
National Aeronautics and Space Administration Washington, D.C. 20546	14. Sponsoring Agency Code

15. Supplementary Notes

16. Abstract

A very-low-density (224 kg/m^3) ablative material, a silicone-phenolic composite, was flight-tested on a recoverable spacecraft launched by a Pacemaker vehicle system; and, in addition, it was tested in an arc-heated wind tunnel at three conditions which encompassed most of the reentry heating conditions of the flight tests. The material was composed, by weight, of 71 percent phenolic spheres, 22.8 percent silicone resin, 2.2 percent catalyst, and 4 percent silica fibers. The tests were conducted to evaluate the ablator performance in both arc-tunnel and flight tests and to determine the predictability of the ablator performance by using computed results from an existing one-dimensional numerical analysis.

The flight-tested ablator experienced only moderate surface recession and retained a smooth surface except for isolated areas where the char was completely removed, probably following reentry and prior to or during recovery.

Analytical results show good agreement between arc-tunnel and flight test results. The thermophysical properties used in the analysis are tabulated herein.

17. Key Words (Suggested by Author(s))	18. Distribution Statement
Very-low-density ablator Silicone-phenolic ablator performance	Unclassified – Unlimited

19. Security Classif. (of this report)	20. Security Classif. (of this page)	21. No. of Pages	22. Price*
Unclassified	Unclassified	31	$3.00

*For sale by the National Technical Information Service, Springfield, Virginia 22151

FLIGHT AND GROUND TESTS OF A VERY-LOW-DENSITY ELASTOMERIC ABLATIVE MATERIAL

By George C. Olsen and Andrew J. Chapman III
Langley Research Center

SUMMARY

A very-low-density (224 kg/m^3) ablative material, a silicone-phenolic composite, was flight-tested on a recoverable spacecraft launched by a Pacemaker vehicle system; and, in addition, it was tested in an arc-heated wind tunnel at three conditions which encompassed most of the reentry heating conditions of the flight tests. The material was composed, by weight, of 71 percent phenolic spheres, 22.8 percent silicone resin, 2.2 percent catalyst, and 4 percent silica fibers. The tests were conducted to evaluate the ablator performance in both arc-tunnel and flight tests and to determine the predictability of the ablator performance by using computed results from an existing one-dimensional numerical analysis.

The flight-tested ablator experienced only moderate surface recession and retained a smooth surface except for isolated areas where the char was completely removed, probably following reentry and prior to or during recovery.

Analytical results show good agreement between arc-tunnel and flight test results. The thermophysical properties used in the analysis are tabulated herein.

INTRODUCTION

Char-forming ablators have been effectively used to protect spacecraft, such as the Apollo command module, from the thermal environment encountered during atmospheric entry. Such materials, having a density of about 400 kg/m^3, have been shown to perform efficiently at heating rates ranging from about 1.0 to 5.5 MW/m^2 (ref. 1). However, at lower heating rates and for long exposures, these materials perform less effectively because of their relatively high thermal conductivity and density. Manned lifting entry vehicles, such as the space shuttle, are expected to experience heating rates of less than 1.0 MW/m^2 over large areas of the vehicle surface. Exposure to these heating rates could last as long as 2000 sec. To protect these vehicles efficiently, very-low-density ($\approx$250 kg/m^3) charring ablators are being developed. Such ablators capable of efficiently performing in this range of flight conditions could effect a significant savings in the weight of the thermal protection system for a lifting entry vehicle.

Tests of several low-density ablative materials, which varied in composition and density, are reported in reference 2. These tests were conducted in an arc-tunnel facility at heating rates ranging from 0.2 MW/m^2 to 0.7 MW/m^2. The results showed that materials with densities as low as 215 kg/m^3 produced chars with good integrity and performed efficiently. However, arc-tunnel tests do not reproduce all of the conditions encountered in flight and there were no flight test data for these materials.

The purpose of the present investigation is to evaluate the performance of a very-low-density ablator in both an arc-heated wind tunnel and a flight test and to determine the predictability of ablator performance by using computed results from an existing one-dimensional numerical analysis (ref. 3). Panels of the material, a silicone-phenolic composite designated MG 36 in reference 2, were fabricated with honeycomb-core reinforcement and a phenolic-glass sheet on the back surface. The ablator composition, by percent weight, was 71 percent phenolic spheres, 22.8 percent silicone resin, 2.2 percent catalyst, and 4 percent silica fibers. The density of the panels was 224 kg/m^3. Detailed descriptions of the material processing and the panel fabrication are presented in appendixes A and B, respectively. Specimens of the material were flight-tested on the afterbody of a recoverable spacecraft launched by a Pacemaker vehicle system. Additional specimens were tested in an arc-tunnel facility over the same heating-rate range expected for the flight test. The results of the arc-tunnel tests are correlated with results from the analysis of reference 3 to obtain certain thermophysical properties which are difficult to measure. The set of thermophysical properties is presented herein. The ground and flight test data are compared with analytical predictions; the data and the comparisons are presented herein.

SYMBOLS

h_e local enthalpy external to boundary layer

h_w local enthalpy of fluid at wall

q_{cw} cold-wall convective heating rate

Q_T total heat load

FLIGHT TEST

Test Vehicle and Ablator Panels

Two ablator panels were flight-tested as part of an experiment flown on a Pacemaker vehicle. The test section of the vehicle was a hemispherically blunted cone with a cylin-

drical afterbody. Its configuration is shown in figure 1 and it is further described in reference 4. The forward portion of the test section, consisting of the spherically blunted cone and part of the cylinder, was thermally protected by a carbon-phenolic material. The remainder of the cylinder was protected by three low-density ablators: the silicone-phenolic composite, a Pyrrone foam, and a phenolic-nylon composite. Two panels of each ablator, machined to 37.8 cm in length and a 60° arc, were mounted in diametrically opposed locations on the cylinder. Cutouts for antenna windows were located in four of the panels in the position shown in figure 1. The performance of the carbon-phenolic material is reported in reference 4 and that of the Pyrrone foam, in reference 5. Results for the two silicone-phenolic panels, which were identified as P-9 and P-12, are given herein. The phenolic-nylon composite did not survive the flight test, presumably because the material was inadequately cured by the experimental dielectric curing process used, and the results are not reported.

As shown in figures 2 and 3, the cylindrical aluminum substructure of the spacecraft was covered with a 6.35-mm layer of phenolic-cork. The cork was bonded to the aluminum substructure with an epoxy-based resin, and the ablator panels were bonded to the cork with a room-temperature-vulcanizing (RTV) silicone-rubber adhesive. The silicone-rubber adhesive was also used to fill the joints between panels. After all panels were installed and the bonds cured, the surface of the heat shield was machined to an outside radius of 12.70 cm.

Each panel was instrumented with in-depth thermocouples mounted in a plug 6.35 mm in diameter, as shown in figure 3. These plugs were made of the same ablative material as the ablator panels and had the same phenolic-cork sublayer. The plugs were bonded, with silicone-rubber adhesive, in holes drilled from the inside of the cylinder to a specified depth from the outside surface. These holes were located on the panel longitudinal center lines and 7.62 cm from the forward edges of the panels. Each plug had two 30-gage chromel-alumel thermocouples located so that one thermocouple would sense the temperature at the back surface of the ablative material and the other thermocouple would sense the temperature at a specified distance from the outside surface of the ablative material. The in-depth measurement was made at 5.08 mm from the outside surface on panel P-9 and at 3.30 mm on panel P-12. The thermocouple beads were located in the center of the plug with the leads running laterally to the plug edges (parallel to the panel surface) and then down the plug sides.

Launch Operations and Flight Environment

The Pacemaker vehicle was launched from the NASA Wallops Station launch facility. The launch vehicle and launch operations are described in references 4 and 5. The Pacemaker vehicle consisted of four stages of solid-propellant rocket motors. The first

two stages were fired on ascent to obtain a maximum altitude of 18 300 m. The third and fourth stages were fired on vehicle descent to obtain a maximum velocity of 3050 m/sec. After fourth stage burnout, the vehicle descended to an altitude of 3048 m where the fourth stage was separated and a parachute was deployed. The payload was lowered to the water 104 km down range from the launch site and recovered. The trajectory data obtained by tracking radar are shown in figure 4. Telemetered accelerometer data and gyro data indicate that the total angle of attack during descent was less than 2.5° and that there was a roll rate of 86.1 deg/sec at third-stage burnout. Thermocouple data from the instrumented test points were telemetered to the ground facility and recorded. The recovered specimens were cross-sectioned and measured to determine surface recessions and pyrolysis-interface recessions.

Measured variations in atmospheric temperature and density are given in reference 4, as well as computed histories of heating rate, pressure, shear stress, and Reynolds number for the instrumented stations on the forward part of the spacecraft. The computed histories of heating rate, pressure, and enthalpy for the ablator-panel thermocouple locations are given in figure 5. All computations were made by utilizing the same methods described in reference 4.

ARC-TUNNEL TESTS

Facility and Test Specimens

The silicone-phenolic ablator was tested in an arc-heated wind tunnel (apparatus B of the Langley entry structures facility). Reference 6 gives a detailed description of the arc-heater system for this facility and reference 7 describes the facility in its present mode of operation.

Arc-tunnel test specimens were prepared from disks, 4 cm in diameter, cut from one of the ablator panels previously described. The disks were bonded to specimen holders with RTV silicone-rubber adhesive and machined to the configuration shown in figure 6. Each specimen was instrumented with a 30-gage chromel-alumel thermocouple mounted on a threaded-plug and post assembly (fig. 6). The thermocouple junction was centered on top of the post, 6.35 mm in diameter, and insulated from it by a silicone-rubber pad. The plug assembly was screwed into the holder until the thermocouple junction was pressed firmly against the phenolic-glass sheet on the back of the specimen.

Heating Environment

Three arc-tunnel stagnation-flow tests (designated tests A, B, and C with corresponding specimens A, B, and C, respectively) were conducted, each with a different set of heating parameters. The heating parameters, shown in table I, were selected to

bracket flight test heating parameters predicted for a preliminary trajectory. However, the trajectory was modified and figure 7 shows comparisons of the heating parameters for the arc-tunnel tests and for the actual flight trajectory. The comparisons show that the ground-test heating rates bracket the peak flight-test heating rates but that the total heat inputs Q_T are lower in the ground tests. They also show that the ground-test pressures bracket the flight-test pressure during high heating (flight time period between 70 and 100 sec) but that the test-stream enthalpies are higher than the flight-test enthalpies. The tests were conducted in an air test stream.

Test Procedure

Prior to the testing of each specimen, the arc tunnel was started and stable operating conditions were established. The cold-wall heating rate was measured by using a thin-skin calorimeter the same shape and size as a specimen. Then the stagnation pressure was measured by using a pressure probe also the same shape and size as a specimen. After these initial measurements, each specimen was inserted into the test stream for a predetermined exposure time. Immediately after withdrawal of the specimen from the test stream, the heating-rate and pressure measurements were repeated. The two measurements were used to obtain average values for these parameters. Following withdrawal, the specimen was allowed to cool in the test chamber at a pressure of approximately 1×10^{-3} atm (1 atm = 101.325 kN/m^2). The specimen thermocouple data were recorded through the exposure time and the thermal soak period for a total of 100 sec. After the tested specimens were cross-sectioned and photographed, they were measured to determine surface recession and pyrolysis-interface recession.

RESULTS AND DISCUSSION

Arc-Tunnel Tests

Posttest photographs, including an oblique surface view and a cross-sectional view of each arc-tunnel test specimen, are shown in figure 8. Specimen A had a smooth surface and a uniform pyrolysis interface. Specimen B exhibited pronounced surface roughness characterized by a cup-like recession in each honeycomb-core cell. This nonuniform recession was probably caused by a combination of accelerated oxidation at the high pressure of test B and differences in thermal conductivity between the ablative material and the more conductive phenolic-glass honeycomb, which would retard oxidation in the vicinity of the honeycomb. Specimen C, tested at a higher heat-transfer rate but lower pressure than specimen B, exhibited less surface roughness, an indication that oxidation was less severe at the lower pressure. Despite surface roughness, specimens B and C had uniform pyrolysis-interface boundaries.

The one-dimensional numerical analysis described in reference 3 was used to calculate the performance of the ablative material for the arc-tunnel test environments. The calculations were made by using the Langley Research Center Digital Computer Charring Ablator Program (CHAP I). In these calculations the mathematical model was applied with the material considered a charring ablator with first-order surface oxidation and a temperature-dependent pyrolysis rate. The phenolic-glass sheet was combined with the high-density bonds and considered a heat sink.

To predict ablator performance, the analysis required environmental parameters including total stream enthalpy, total pressure, and cold-wall heat-transfer rate. The analysis also required a set of material thermophysical properties. One of the purposes of the ground tests was to provide data with which to assemble a set of thermophysical properties. These properties could then be used to calculate the performance of the ablator over a range of conditions that included the arc-tunnel tests and the flight test. Table II lists the properties which provide good correlation between the calculated and the ground-test performance and identifies their sources. Many of the properties are measured values, obtained by using either the ablator from the present investigation or a very similar one. Certain properties were calculated by using the chemical-equilibrium analysis of reference 8. Other properties, which were difficult to measure or calculate, were derived by iterating inputs to the analysis of reference 3 until the computed results matched the test results over the range of conditions reported herein.

When the CHAP I program is used, the normal reference base for the heating rate and for the enthalpies is 300 K. However, in this case, it was necessary to change the reference base to 0 K to avoid the mathematical singularity which develops in the net convective heating-rate term $q_{cw}\left(1 - \frac{h_w}{h_e}\right)$ (from eq. (13), ref. 3) when h_e approaches zero during cooling. Changing the reference base to 0 K removes this mathematical singularity from the domain of interest without changing the value of the term; that is,

$$q_{cw}\left(1 - \frac{h_w}{h_e}\right) = q'_{cw}\left(1 - \frac{h'_w}{h'_e}\right)$$

where the primed quantities refer to the 0 K base and the unprimed quantities refer to the 300 K base. The change was made as follows:

$$h'_e = h_e + \Delta h$$

$$h'_w = h_w + \Delta h$$

$$q'_{cw} = \frac{h'_e}{h_e} q_{cw}$$

where Δh, the difference in the enthalpy of dry air at 0 K and at 300 K, was taken to be 0.3 MJ/kg from reference 9.

Figure 9 shows the measured total surface and pyrolysis-interface recessions compared with the calculated surface and pyrolysis-interface recession histories. The measured quantities are mean values for each specimen. The deviations from the mean, due to surface roughness or poorly defined interface positions, are estimated to be within ±0.2 mm except that the deviation for the surface-recession measurement of specimen B is estimated to be within ±0.8 mm.

Comparisons of measured and calculated back-surface temperature histories are presented in figure 10. The measured temperatures of specimens A and B show an early rise followed by a period of constant temperature. Behavior of this type is reported in reference 10 and is attributed to water vapor formed as a pyrolysis product. This vapor permeates the virgin material and causes a temperature rise. The back-surface temperature then remains nearly constant until conduction from the surface causes it to rise again. The effect is not discernible in specimen C; however, this specimen had a delamination between the phenolic-glass honeycomb and the phenolic-glass sheet which would cause a delay in the thermocouple response. The delamination can be seen in the cross-sectional photograph of the specimen in figure 8(c). The vapor mechanism is not accounted for in the analytical model and, as a result, the calculated temperatures do not show the early rise and the period of uniform temperature. The calculated results agree closely with the measured temperatures during the early thermal soak period of tests A and B. The difference of 10 K between the measured and calculated temperatures for specimen C during this period is also attributed to the delamination between the honeycomb and the phenolic-glass sheet.

In the later stages of each test (beyond 50 sec) a difference of not more than 20 K between the measured and calculated responses is evident. The difference is attributed to heat conduction to the thermocouple location from the periphery of the phenolic-glass sheet, which was in contact with the high-temperature char layer. This lateral heat conduction cannot be accounted for in the one-dimensional mathematical model.

Flight Test

Photographs of the flight test panels on the recovered spacecraft are shown in figure 11(a); photographs of the recovered panels after cross-sectioning, in figure 11(b). The photographs of the surfaces of panels P-9 and P-12 show areas of char which remained intact and maintained a smooth surface (much smoother than arc-tunnel tests B and C). These photographs also show areas where the char was detached and a roughened lower surface was left. The randomness of the damaged-char areas, the rough surfaces exposed, and the lack of perturbations in the pyrolysis-interface recession below the

damage indicate that the char was detached after heating ended. The damage probably occurred when the payload was subjected to the shocks of parachute deployment, water impact, sea-water exposure, and/or recovery.

The one-dimensional analysis and computer program used to calculate the material performance for the arc-tunnel tests were also used to calculate the material performance for the flight test. In addition to the modeling considerations used for the arc-tunnel tests, the flight-test modeling considered the phenolic-cork sublayer as a layer of insulation and the aluminum substructure as another heat sink. The flight environmental parameters and the set of thermophysical properties assembled in conjunction with the arc-tunnel tests were used to make the calculations.

Measured surface and pyrolysis-interface recessions for the areas of undamaged char are presented in figure 12 and compared with calculated recession histories. The measurement uncertainty for the flight-specimen recessions is ±0.25 mm. Within this uncertainty band the calculated recessions agree with the measured recessions.

Figure 13 presents the temperature histories measured by the in-depth and back-surface thermocouples located in each specimen and also the temperature histories calculated for these thermocouple locations. Comparisons of the flight measured and the calculated temperature histories show good agreement, with minor exceptions. The calculated back-surface temperature history falls within the scatter of experimental measurements for both panels. Again, as in the ground tests, the measured back-surface temperature histories show the early temperature rise and constant-temperature period, attributed to a vapor layer. The calculated and measured temperature histories for the panel P-9 in-depth thermocouple agree within 2 percent during the time the temperature is increasing. Shortly after the temperature begins to decrease the flight-test measurements show an unexplained shift in the temperature history for panel P-9. A similar shift is reported in reference 10. The shift may have been due to a thermocouple malfunction but the exact cause is unknown. Comparison of the measured and calculated data for the in-depth thermocouples on panel P-12 shows good agreement for 85 sec, after which the measured data show a change in the rate of temperature increase that leads to a 14 percent difference between measured and calculated values. However, based on the calculated pyrolysis-interface recession (fig. 12), it is noted that at approximately 85 sec the pyrolysis interface passed the thermocouple location and beyond that time the thermocouple was measuring the char temperature. Because the char is an electrical conductor and can interfere with the thermocouple outputs, the temperature measurements beyond 85 sec are not accurate (ref. 10). The unexplained shift during the thermal soak period also occurred in the measured temperature history for panel P-12.

CONCLUDING REMARKS

A very-low-density (224 kg/m^3) ablative material, a silicone-phenolic composite, was flight-tested on a recoverable spacecraft launched by a Pacemaker vehicle system. In addition, this ablative material was tested in an arc-heated wind tunnel at three conditions which encompassed most of the reentry heating conditions of the flight test.

A set of thermophysical properties was developed for the silicone-phenolic ablative material. These properties were based in part on the ground-test results. Calculations, in which these properties were used, show good agreement with measured surface recession, pyrolysis-interface recession, and temperature histories for both ground and flight tests.

The silicone-phenolic ablator performed in a predictable manner during the flight test. The material experienced moderate surface recession and the char layer maintained a smooth surface except for certain areas where the char layer was detached, probably during the period between parachute deployment and recovery of the flight vehicle from the ocean. These flight data show that very-low-density silicone-phenolic ablative materials can withstand heating rates and pressures associated with manned lifting entry vehicles. Further, these test data show that surface and pyrolysis-interface recessions and temperature histories for this material can be predicted with good accuracy.

Langley Research Center,
National Aeronautics and Space Administration,
Hampton, Va., September 19, 1972.

APPENDIX A

MATERIAL PROCESSING

The silicone-phenolic-composite ablator used in this study had a composition, by percent weight, of 71.0 percent phenolic-spheres filler, 22.8 percent silicone resin, 2.2 percent catalyst, and 4 percent silica fibers.

Prior to mixing, the phenolic-spheres filler was processed separately by screening through a 20-mesh screen into a solids processor and drying for 3 hours at a temperature of 366 K and a pressure of 3.33 kN/m^2 while the processor hopper rotated at 8 rpm. The processor was allowed to cool to 310 K and the dried phenolic spheres were discharged into a solvent-cleaned polyethylene container. The container was sealed to prevent absorption of moisture by the phenolic spheres.

The silicone resin and the catalyst were combined and hand mixed for 5 min. The mixed liquid was poured into a vertical cone mechanical mixer and the silica fibers were added to this mix. The mixer was operated in 5-min forward and reverse rotation cycles and with a 15-rpm blade speed. The mixing continued until the silica fibers were thoroughly wetted and uniformly dispersed in the liquid components. With the mixer still operating, the dried phenolic spheres were placed in the mixer hopper and discharged into the mixing chamber. The total mechanical mixing time was 45 min. The total weight of the processed ingredients was 300 grams.

APPENDIX B

PANEL FABRICATION

Phenolic-glass sheets, 0.5 mm thick, were formed in a cylindrical shape (75° arc with a radius of 11.75 cm and 41.9 cm long) by laying up two plies of preimpregnated phenolic-glass cloth, with warps perpendicular, on a prepared mold base. The assembly was vacuum bagged and cured in an autoclave at elevated temperature and reduced pressure. Following cooling, the phenolic-glass sheet was cleaned and primed according to standard procedures. A phenolic-glass honeycomb core, 1.27 cm thick with 0.95 cm cells, was also cleaned and primed. The sheet and honeycomb were bonded together by using a film adhesive and a bonding fixture employing pressure plates. The assembled bonding fixture was placed in an air-circulating oven and the bond cured at elevated temperature. The cells of the honeycomb were wetted with the silicone resin and the assembly placed in a prepared molding fixture. The processed ablative material was placed on top of the honeycomb and hand screeded into the cells; additional material was added to provide a 1.27-cm overburden. The mold was vacuum bagged and the material was vacuum molded at a pressure of 0.33 kN/m^2. The vacuum was removed and the 1.27-cm overburden replaced. After the vacuum bag was replaced, the assembly was placed in an air-circulating oven where the material was cured at a pressure of 0.33 kN/m^2 and a temperature of 327 K for 1 hour. Atmospheric pressure was restored while the temperature was maintained at 327 K for 15 additional hours. The molded panels were postcured in an air-circulating oven at 373 K for 8 hours.

REFERENCES

1. Swann, Robert T.; Brewer, William D.; and Clark, Ronald K.: Effect of Composition, Density, and Environment on the Ablative Performance of Phenolic Nylon. NASA TN D-3908, 1967.
2. Howell, William E.: Ablative Performance of Various Low-Density Elastomeric Composites. NASA TN D-6130, 1971.
3. Swann, Robert T.; Pittman, Claud M.; and Smith, James C.: One-Dimensional Numerical Analysis of the Transient Response of Thermal Protection Systems. NASA TN D-2976, 1965.
4. Walton, Thomas E., Jr.; and Witte, William G.: Flight Test of Carbon-Phenolic on a Spacecraft Launched by the Pacemaker Vehicle System. NASA TM X-2504, 1972.
5. McLain, Allen G.; and Kelliher, Warren C.: Flight- and Ground-Test Evaluation of Pyrrone Foams. NASA TN D-6711, 1972.
6. Brown, Ronald D.; and Fowler, Bruce: Enthalpy Calculated From Pressure and Flow-Rate Measurements in High-Temperature Subsonic Streams. NASA TN D-3013, 1965.
7. Moss, James N.; and Howell, William E.: A Study of the Performance of Low-Density Phenolic-Nylon Ablators. NASA TN D-5257, 1969.
8. Stroud, C. W.; and Brinkley, Kay L.: Chemical Equilibrium of Ablation Materials Including Condensed Species. NASA TN D-5391, 1969.
9. Eshbach, Ovid W., ed.: Handbook of Engineering Fundamentals. Second ed., John Wiley & Sons, Inc., c.1952.
10. Dow, Marvin B.; Bush, Harold G.; and Tompkins, Stephen S.: Analysis of the Supercircular Reentry Performance of a Low-Density Phenolic-Nylon Ablator. NASA TM X-1577, 1968.
11. Smyly, E. D.; Swoger, W. F.; and Pears, C. D.: Properties of Ablation and Insulation Materials. Vol. III: Thermal and Mechanical Properties of Low-Density Phenolic-Nylon and Silicone-Phenolic Ablators. Contract NAS 1-7732-1, Southern Res. Inst., June 1971. (Available as NASA CR-111909.)

TABLE I.- ARC-TUNNEL TEST CONDITIONS

Test	Stagnation-point cold-wall heating rate,[a] MW/m^2	Total test-stream enthalpy,[a] MJ/kg	Stagnation pressure, atm	Exposure time, sec
A	0.565	4.77	0.082	18.9
B	1.02	5.99	.17	13.7
C	1.27	9.31	.10	9.6

[a] Enthalpy zero base at 300 K.

TABLE II. - THERMOPHYSICAL PROPERTIES OF VERY-LOW-DENSITY ELASTOMERIC ABLATOR

[Data sources in footnotes]

(a) Uncharred material

Density, kg/m^3	[a] 224
Effective heat of pyrolysis, kJ/kg	[b] 813
Specific reaction-rate constant for pyrolysis, kg/m^2-sec-atm	[b] 3.46×10^{14}
Activation temperature for pyrolysis, K	[b] 3.44×10^4
Specific heat of gaseous products of pyrolysis, kJ/kg-K –	
At 300 K	[c] 2.21
At 556 K	[c] 3.10
At 694 K	[c] 3.56
At 833 K	[c] 4.01
At 1000 K	[c] 4.48
At 1111 K	[c] 4.73
At 1250 K	[c] 4.99
At 1389 K	[c] 5.24
At 1528 K	[c] 5.44
At 1667 K	[c] 5.60
At 1944 K	[c] 5.85
At 2222 K	[c] 5.98
Specific heat, kJ/kg-K –	
At 278 K	[d] 1.39
At 350 K	[d] 1.51
At 400 K	[d] 1.58
At 450 K	[d] 1.64
At 500 K	[d] 1.71
At 639 K	[e] 1.89
At 833 K	[e] 2.09
At 944 K	[e] 2.21
At 1111 K	[e] 2.30
Thermal conductivity, W/m-K –	
At 278 K	[d] 0.056
At 333 K	[d] 0.058
At 444 K	[d] 0.057
At 556 K	[e] 0.055
At 778 K	[e] 0.052
At 889 K	[e] 0.05
At 1111 K	[e] 0.047

TABLE II. - THERMOPHYSICAL PROPERTIES OF VERY-LOW-DENSITY ELASTOMERIC ABLATOR – Concluded

(b) Charred material

Density, kg/m^3	[b] 128.1
Surface emittance	[b] 0.8
Heat of combustion of char, kJ/kg	[f] 8833
Specific reaction-rate constant for oxidation, kg/m^2-sec-atm	[f] 9.76×10^8
Activation temperature for oxidation, K	[f] 3.33×10^4
Weight of char removed per unit weight of oxygen	[f] 0.83
Specific heat, kJ/kg-K –	
At 278 K	[e] 0.50
At 556 K	[d] 0.67
At 833 K	[d] 1.09
At 1111 K	[d] 1.76
At 1389 K	[d] 2.38
At 1667 K	[d] 2.89
At 1944 K	[d] 3.22
Thermal conductivity, W/m-K –	
At 278 K	[b] 0.124
At 556 K	[b] 0.156
At 833 K	[b] 0.249
At 1111 K	[b] 0.404
At 1667 K	[b] 0.684
At 2222 K	[b] 0.995

[a] Measured.
[b] Computer correlated.
[c] Calculated from chemical-equilibrium analysis (ref. 8).
[d] Based on measured values for similar material (ref. 11).
[e] Extrapolated from measured values for similar material (ref. 11).
[f] Based on unpublished data.

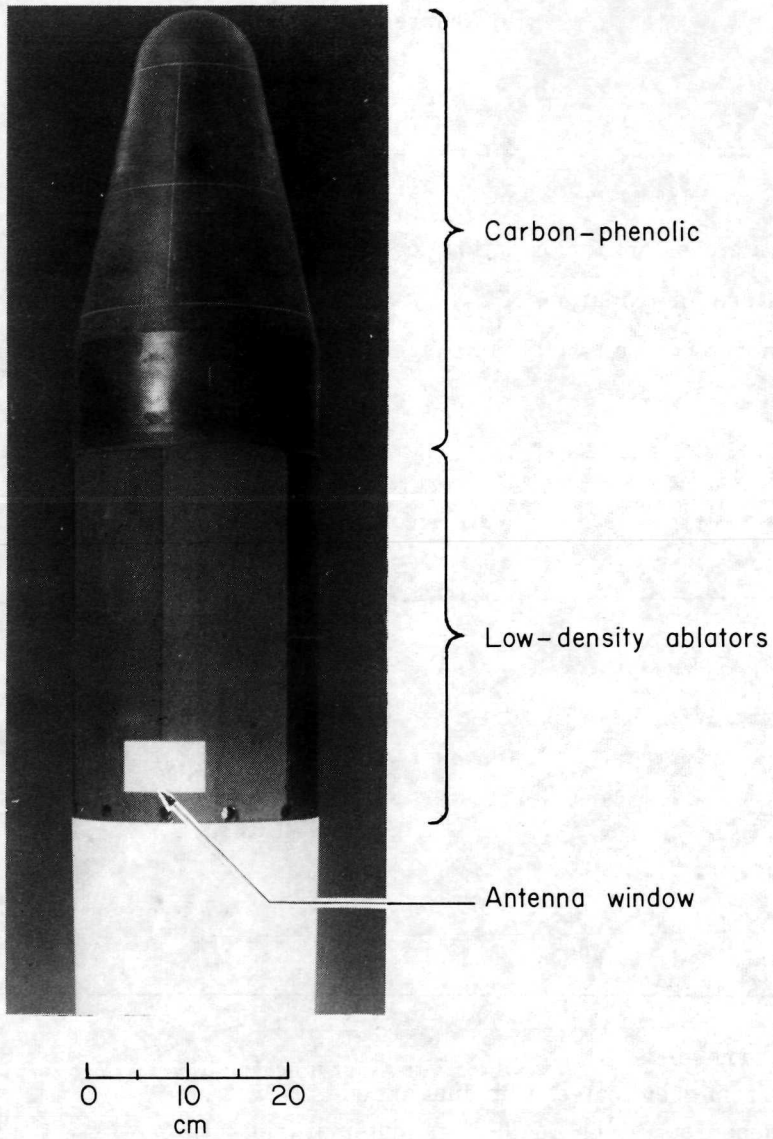

L-72-6503

Figure 1.- Photograph of test section of flight test vehicle.

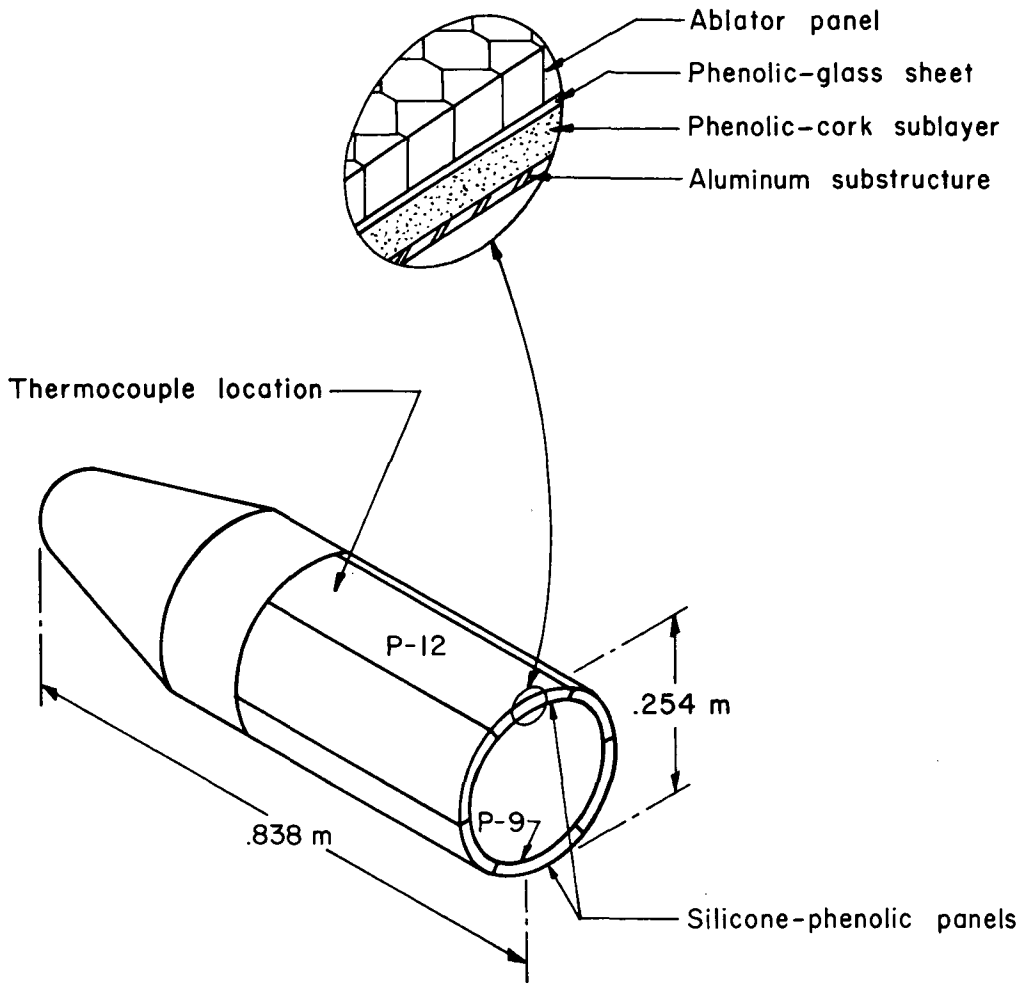

Figure 2.- Schematic diagram of test section of flight test vehicle.

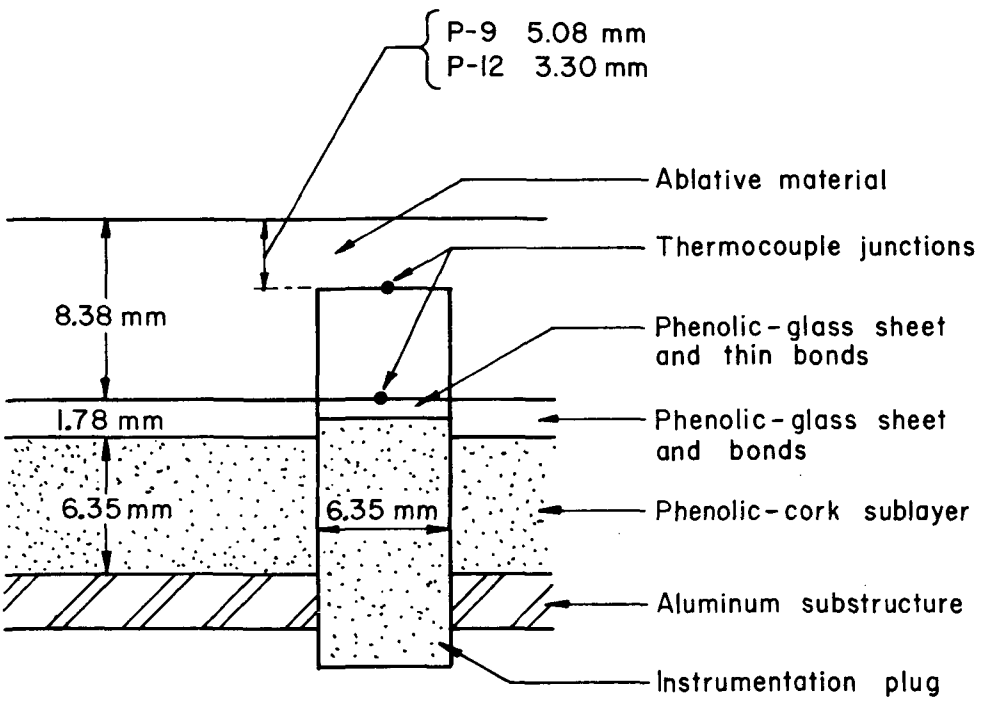

Figure 3.- Flight-test panel instrumentation.

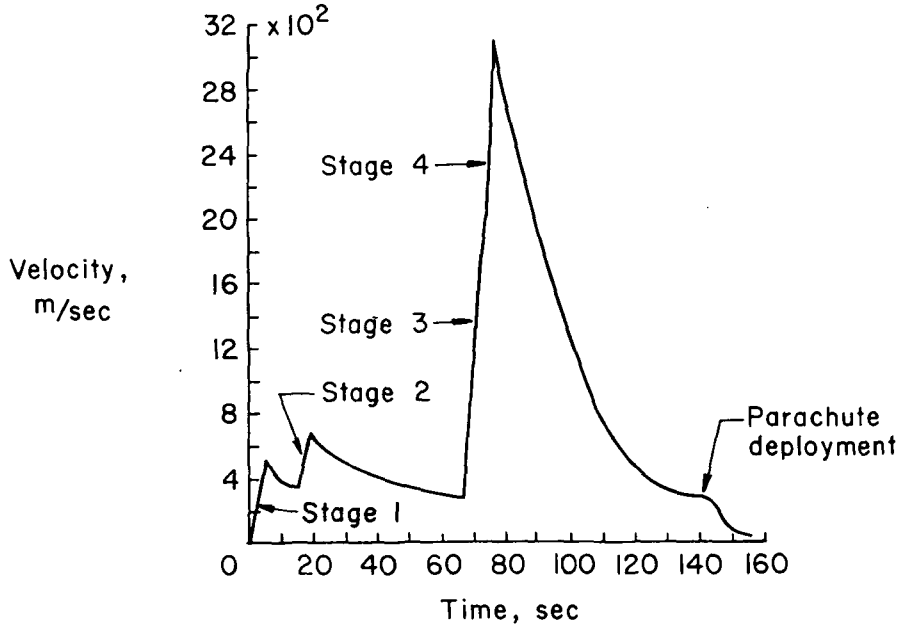

(a) Velocity history.

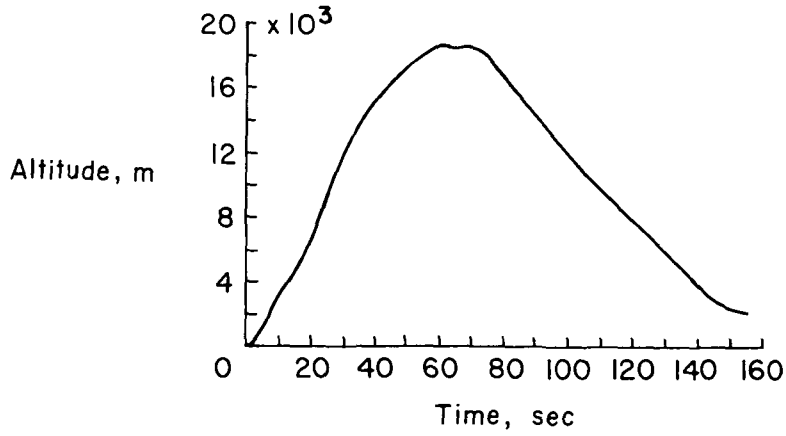

(b) Altitude history.

Figure 4.- Flight test trajectory.

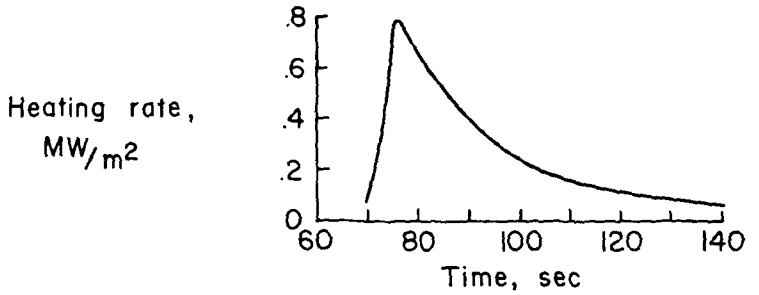

(a) Heating-rate history.

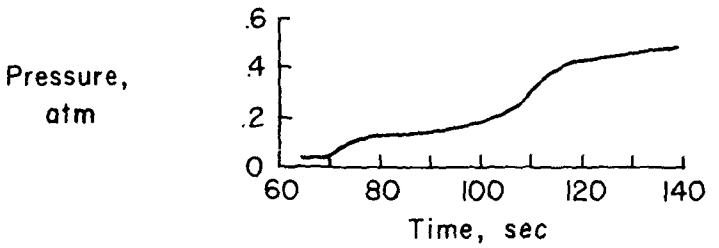

(b) Pressure history.

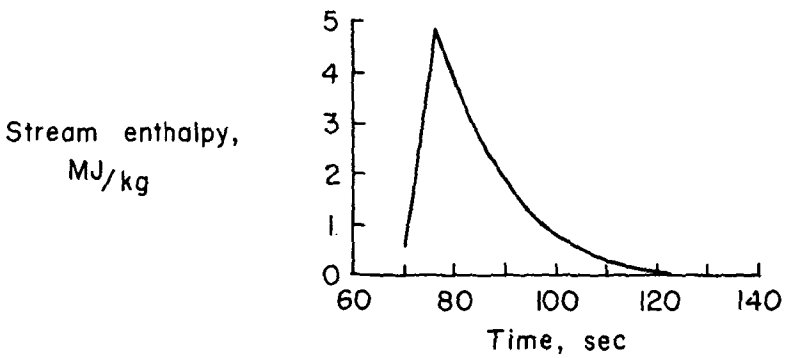

(c) Stream-enthalpy history.

Figure 5.- Flight test conditions at thermocouple locations.

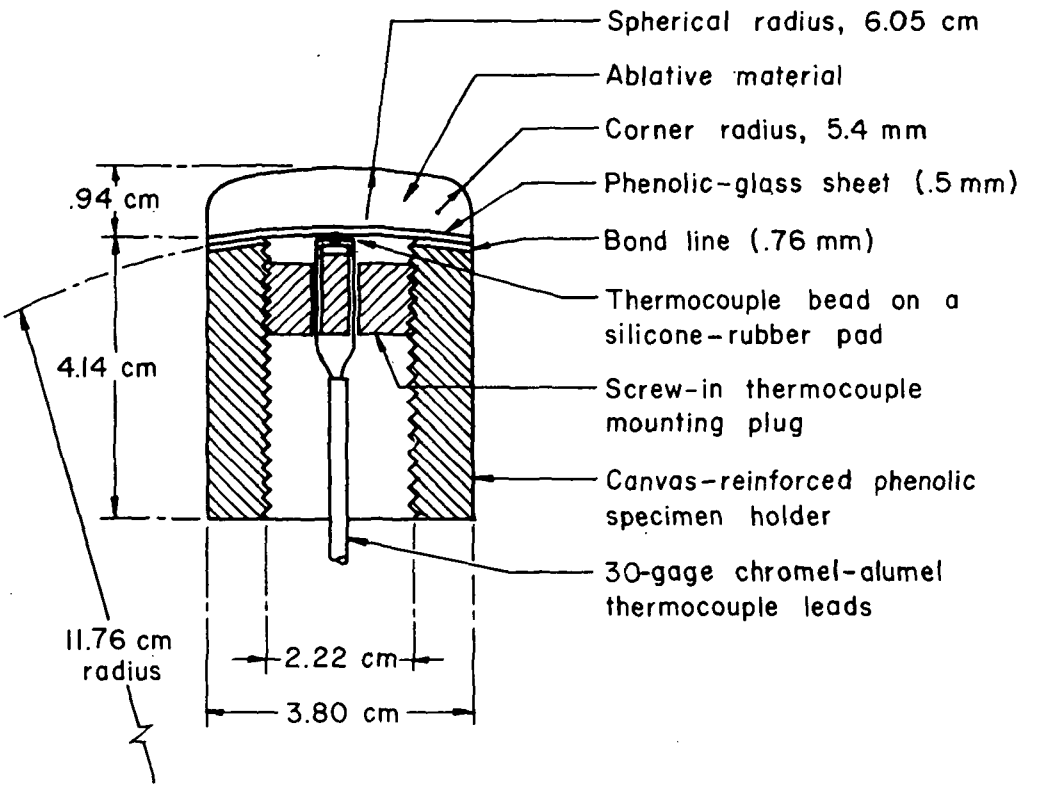

Figure 6.- Arc-tunnel test specimen.

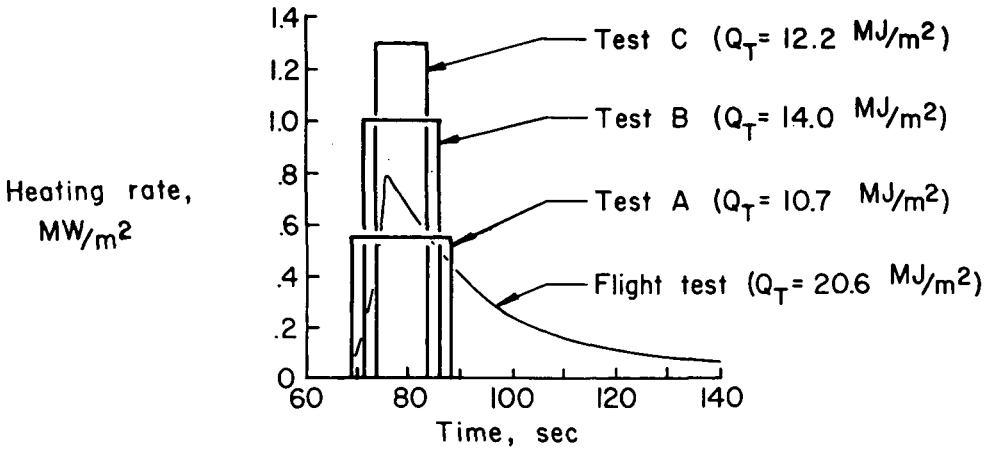

(a) Heating rate.

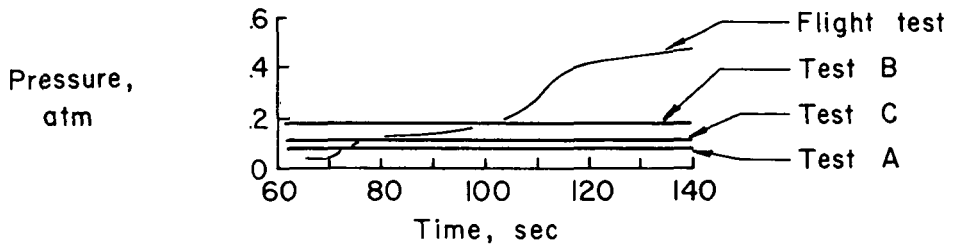

(b) Pressure.

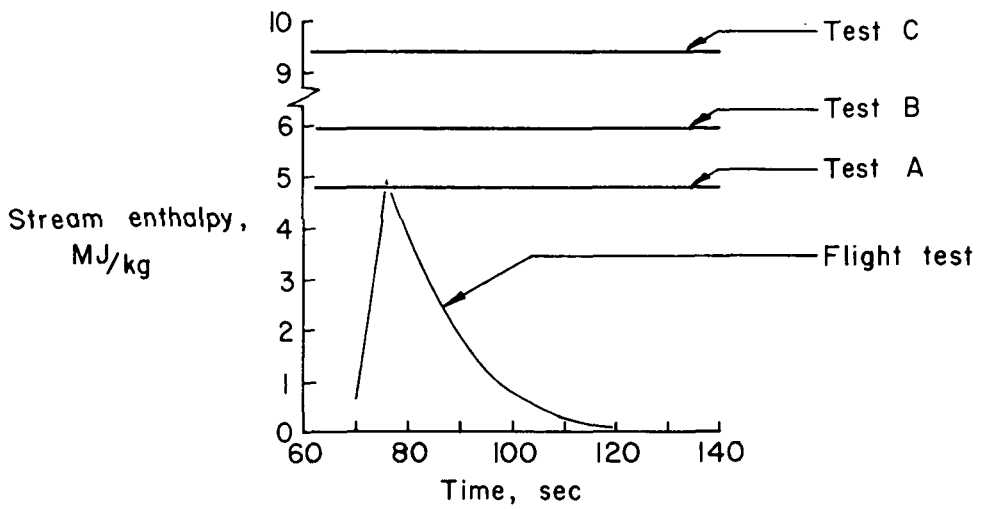

(c) Stream enthalpy.

Figure 7.- Comparisons of flight and arc-tunnel test conditions.

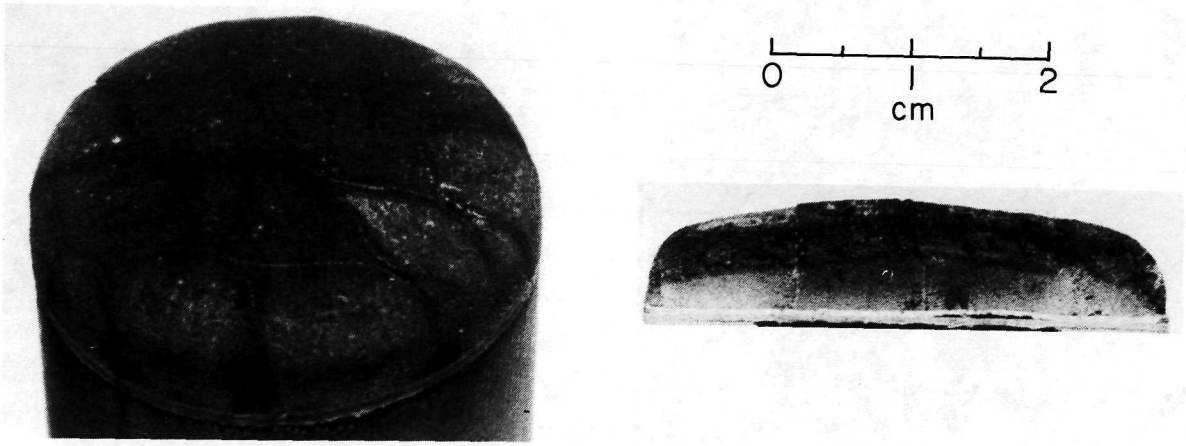

(a) Test specimen A.

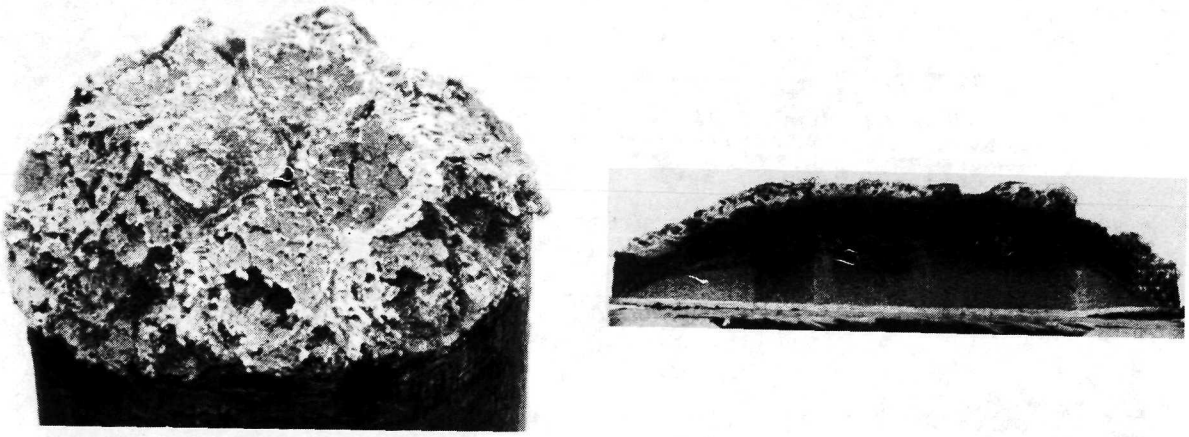

(b) Test specimen B.

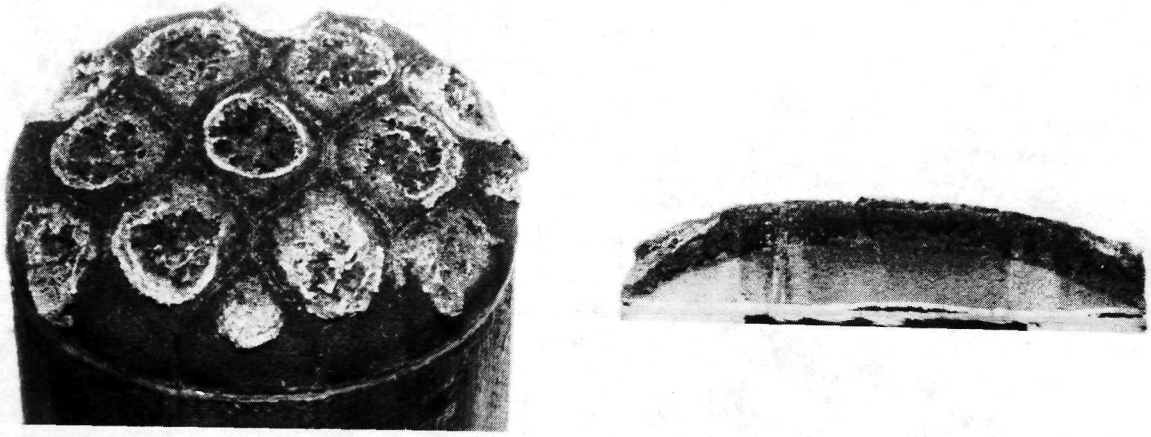

(c) Test specimen C.

L-72-6504

Figure 8.- Posttest photographs of arc-tunnel test specimens.

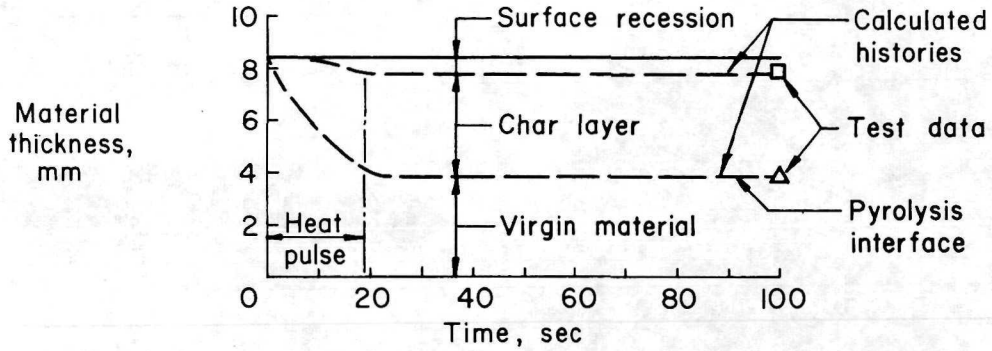

(a) Test specimen A.

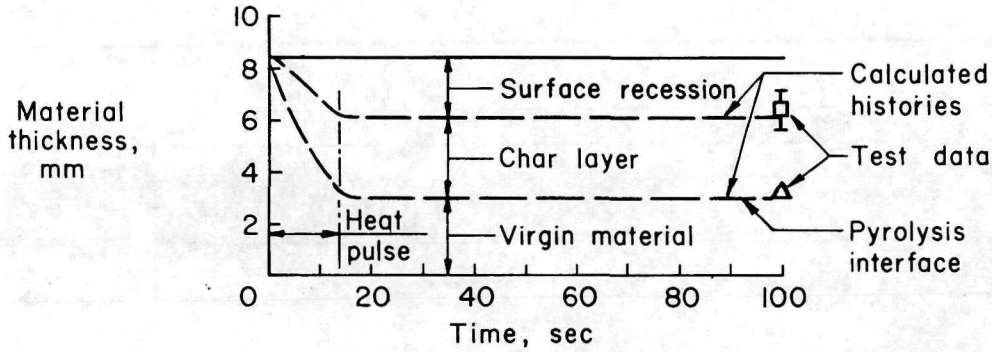

(b) Test specimen B.

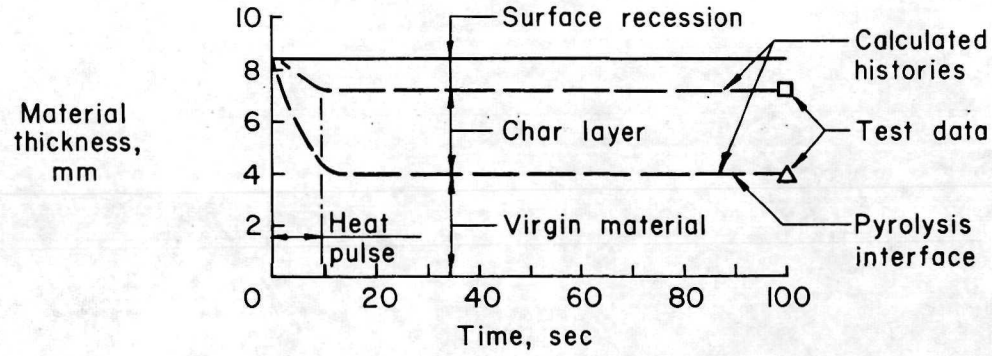

(c) Test specimen C.

Figure 9.- Comparisons of measured and calculated recession data for arc-tunnel test specimens.

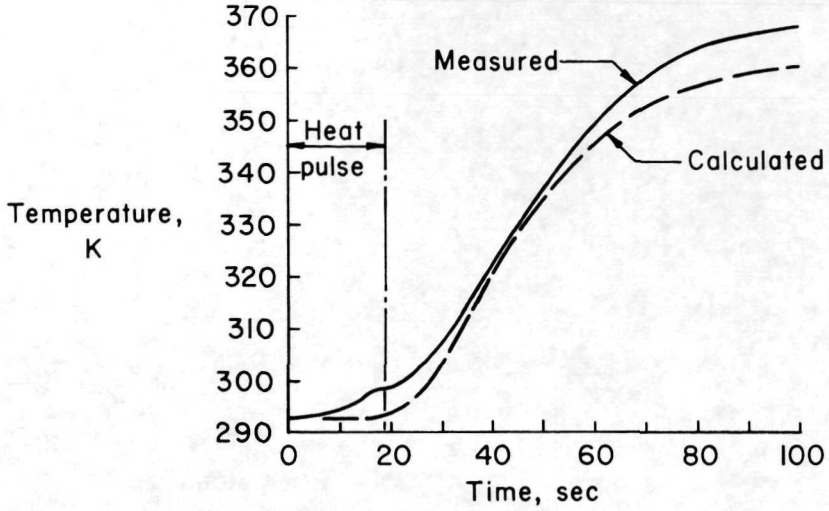

(a) Test specimen A.

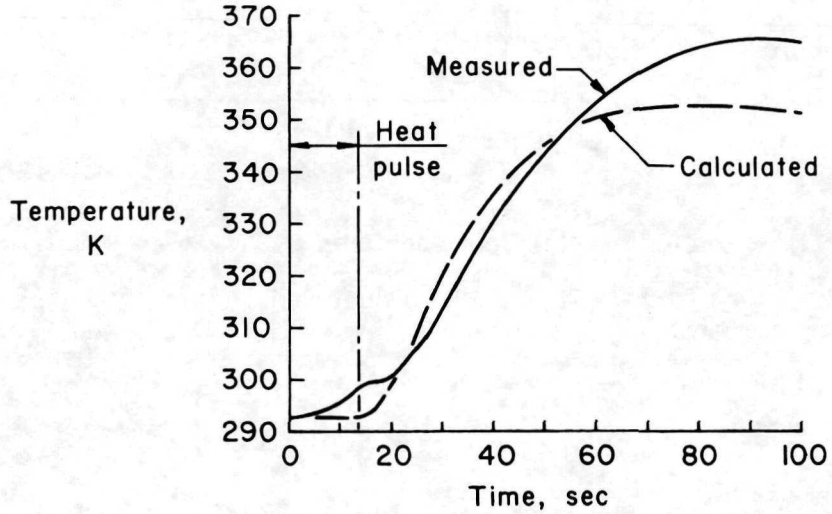

(b) Test specimen B.

Figure 10.- Comparisons of measured and calculated back-surface temperature histories for arc-tunnel test specimens.

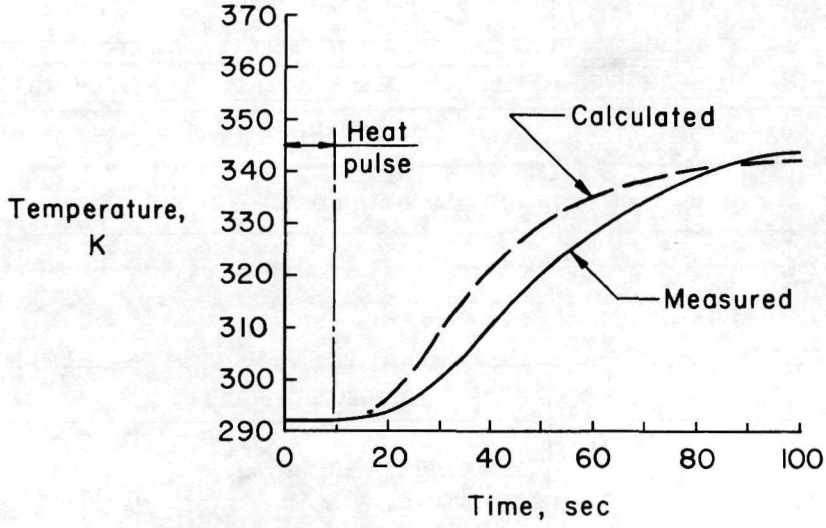

(c) Test specimen C.

Figure 10.- Concluded.

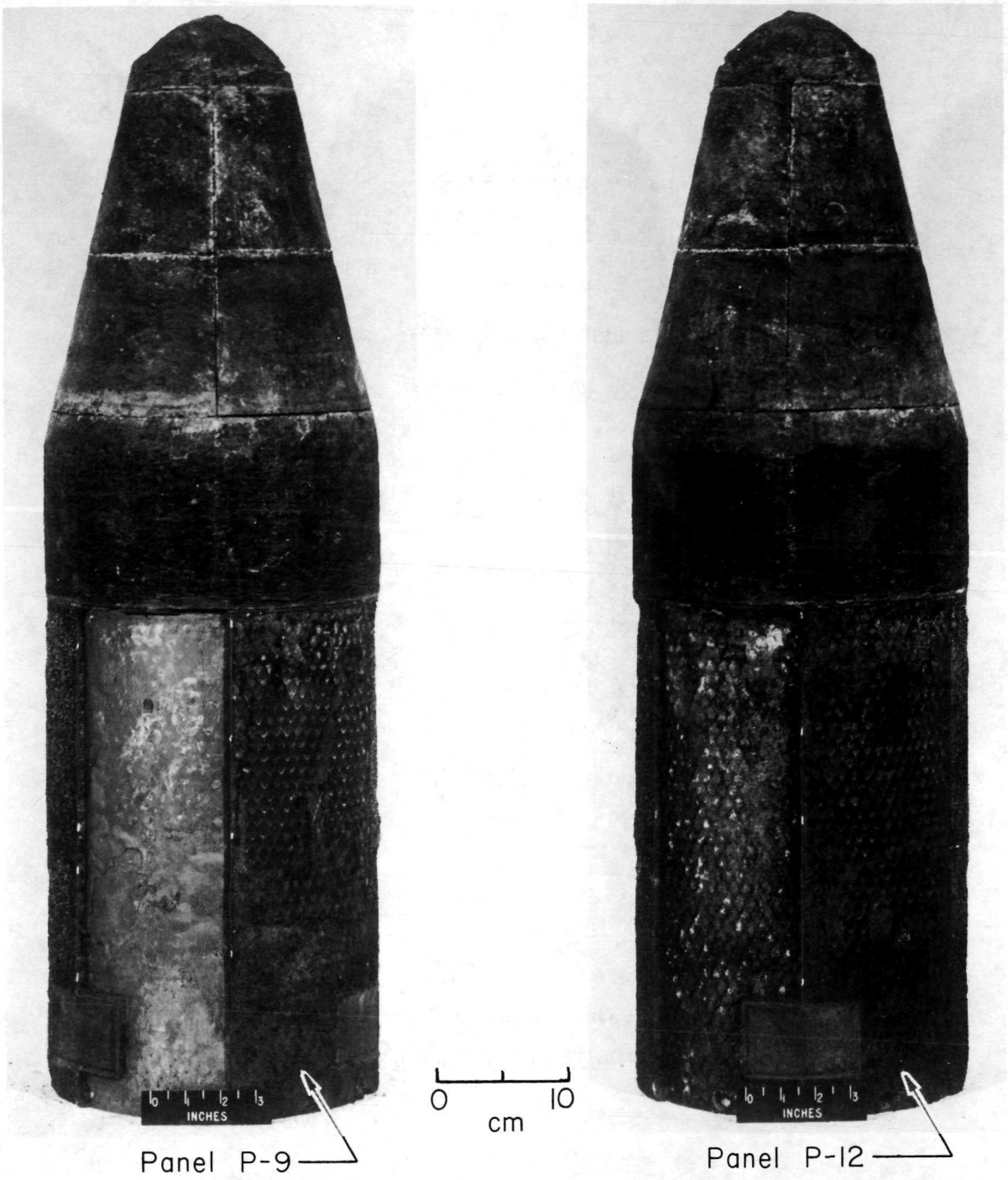

(a) Surface views.

L-72-6505

Figure 11.- Photographs of recovered flight test specimens.

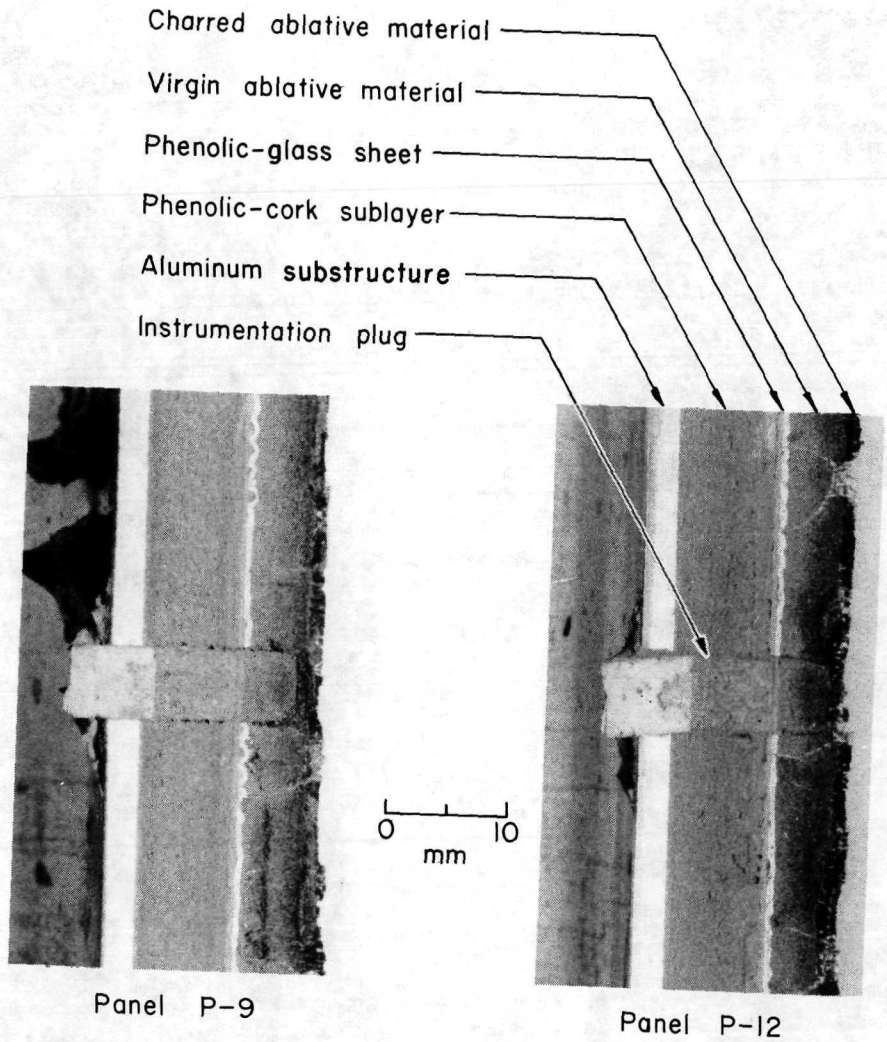

(b) Cross-sectional views. L-72-6506

Figure 11.- Concluded.

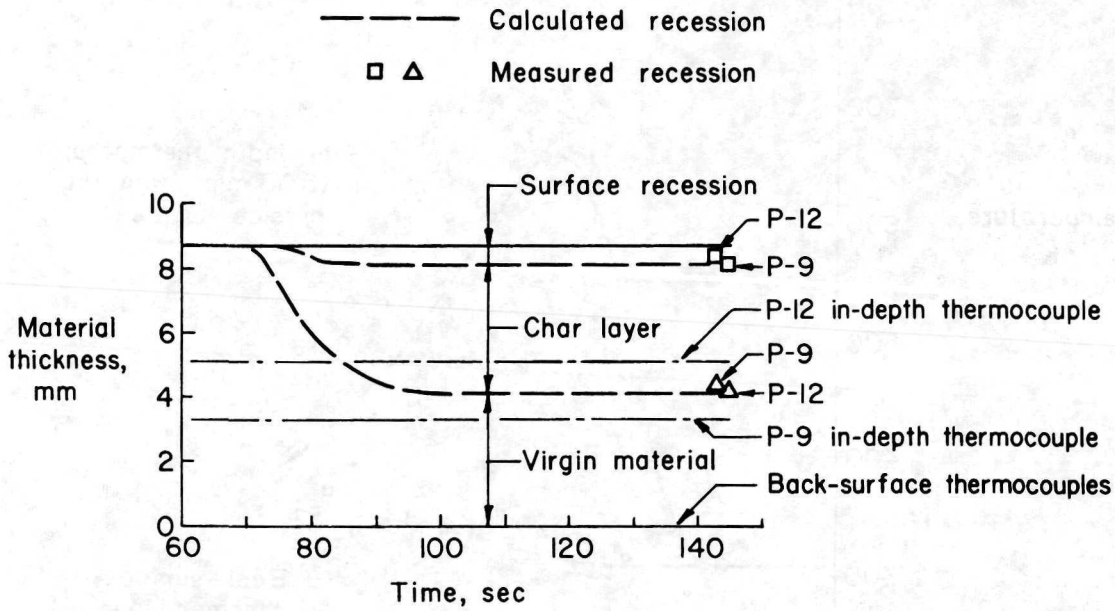

Figure 12.- Comparisons of calculated and measured recession data for flight test specimens.

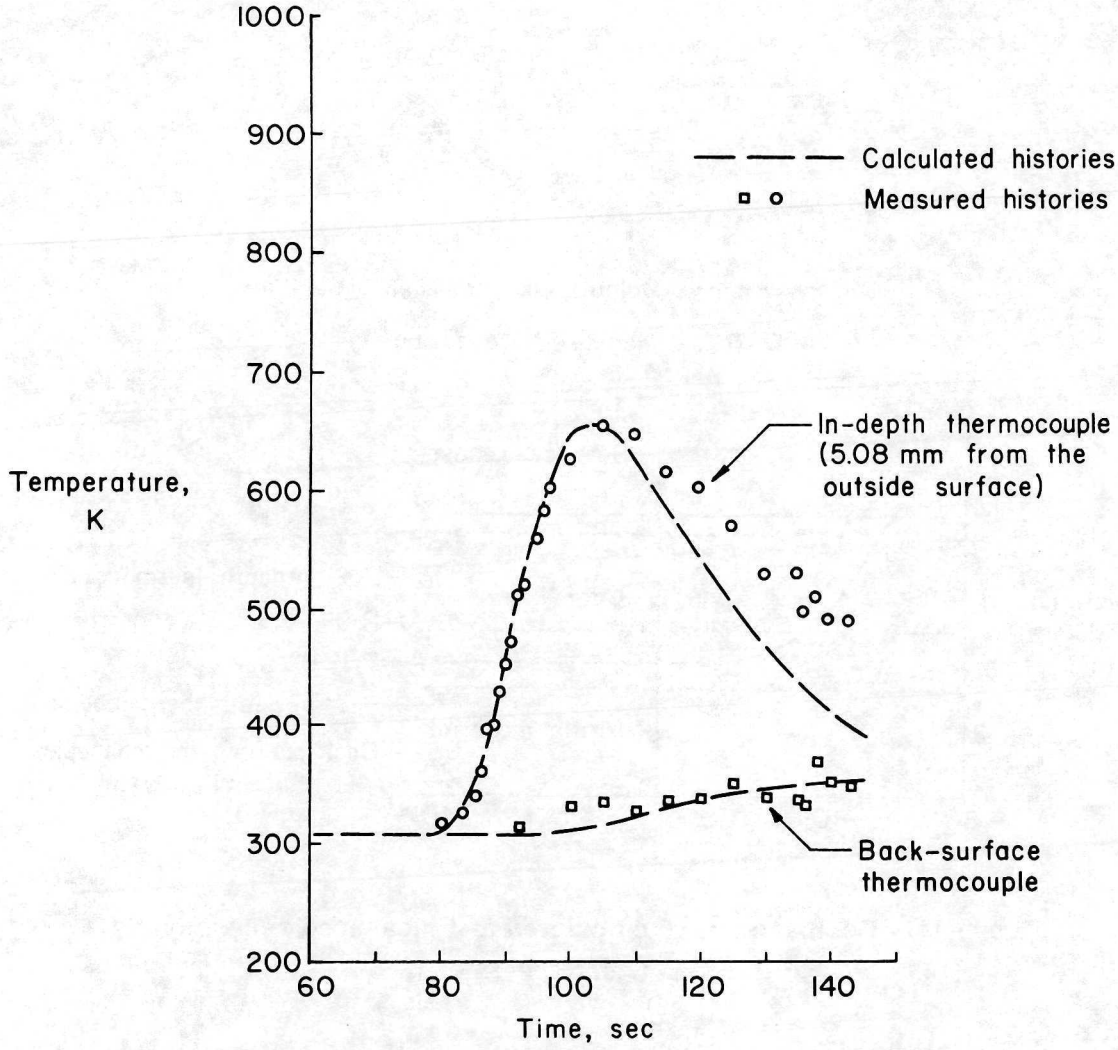

(a) Panel P-9.

Figure 13.- Comparisons of measured and calculated temperature histories for flight test specimens.

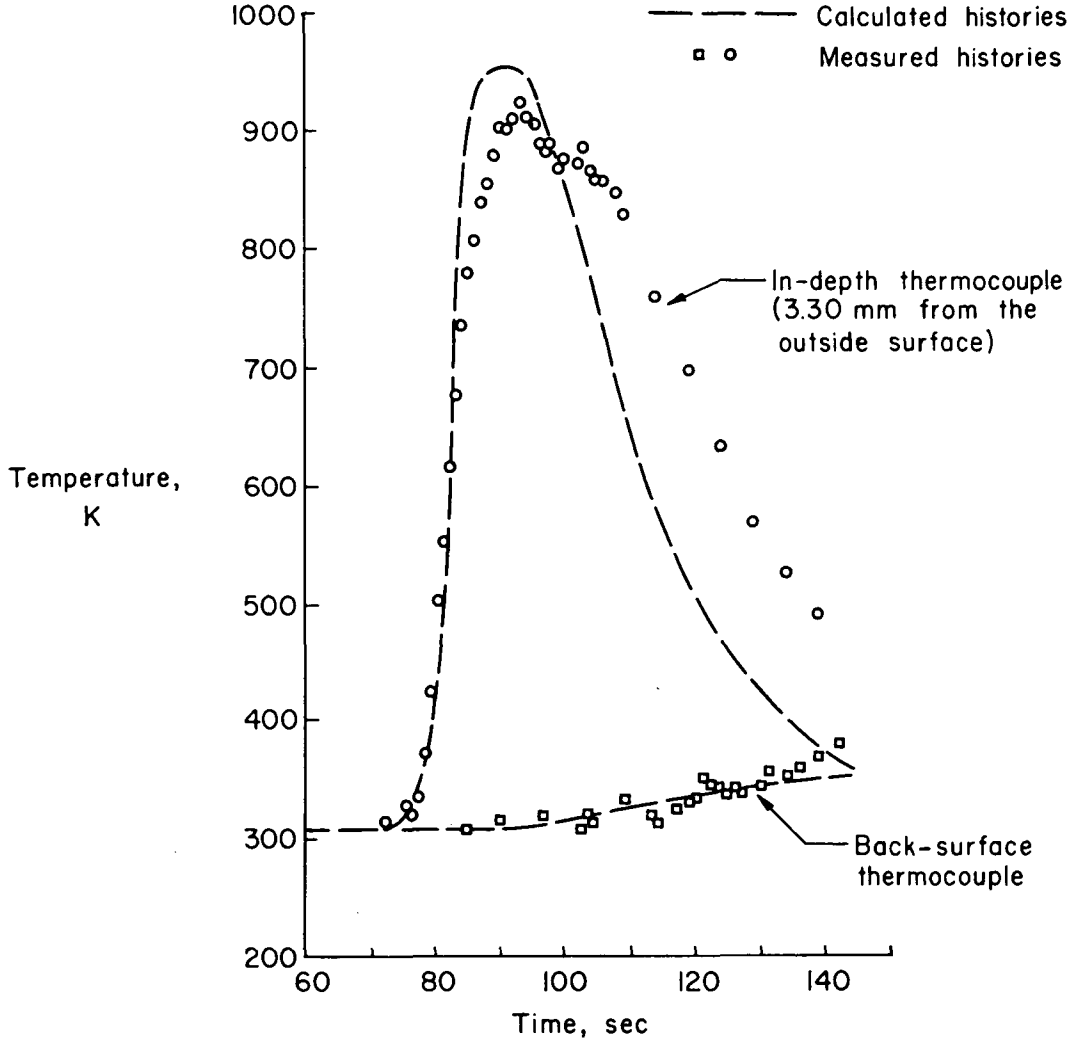

(b) Panel P-12.

Figure 13.- Concluded.

NATIONAL AERONAUTICS AND SPACE ADMINISTRATION
WASHINGTON, D.C. 20546

OFFICIAL BUSINESS
PENALTY FOR PRIVATE USE $300

SPECIAL FOURTH-CLASS RATE
BOOK

POSTAGE AND FEES PAID
NATIONAL AERONAUTICS AND
SPACE ADMINISTRATION
451

U.S.MAIL

POSTMASTER: If Undeliverable (Section 158 Postal Manual) Do Not Return

"The aeronautical and space activities of the United States shall be conducted so as to contribute . . . to the expansion of human knowledge of phenomena in the atmosphere and space. The Administration shall provide for the widest practicable and appropriate dissemination of information concerning its activities and the results thereof."

—NATIONAL AERONAUTICS AND SPACE ACT OF 1958

NASA SCIENTIFIC AND TECHNICAL PUBLICATIONS

TECHNICAL REPORTS: Scientific and technical information considered important, complete, and a lasting contribution to existing knowledge.

TECHNICAL NOTES: Information less broad in scope but nevertheless of importance as a contribution to existing knowledge.

TECHNICAL MEMORANDUMS: Information receiving limited distribution because of preliminary data, security classification, or other reasons. Also includes conference proceedings with either limited or unlimited distribution.

CONTRACTOR REPORTS: Scientific and technical information generated under a NASA contract or grant and considered an important contribution to existing knowledge.

TECHNICAL TRANSLATIONS: Information published in a foreign language considered to merit NASA distribution in English.

SPECIAL PUBLICATIONS: Information derived from or of value to NASA activities. Publications include final reports of major projects, monographs, data compilations, handbooks, sourcebooks, and special bibliographies.

TECHNOLOGY UTILIZATION PUBLICATIONS: Information on technology used by NASA that may be of particular interest in commercial and other non-aerospace applications. Publications include Tech Briefs, Technology Utilization Reports and Technology Surveys.

Details on the availability of these publications may be obtained from:

SCIENTIFIC AND TECHNICAL INFORMATION OFFICE

NATIONAL AERONAUTICS AND SPACE ADMINISTRATION

Washington, D.C. 20546